Short-term forecasting of life-threatening cardiac arrhythmias based on symbolic dynamics and finite-time growth rates

Niels Wessel,[1,2,*] Christine Ziehmann,[2] Jürgen Kurths,[2] Udo Meyerfeldt,[3] Alexander Schirdewan,[3] and Andreas Voss[1]
[1]*University of Applied Sciences Jena, Tatzendpromenade 1b, 07745 Jena, Germany*
[2]*University Potsdam, Postfach 601553, 14415 Potsdam, Germany*
[3]*Franz-Volhard-Hospital, Wiltbergstrasse 50, 13125 Berlin, Germany*
(Received 21 December 1998; revised manuscript received 26 July 1999)

Ventricular tachycardia or fibrillation (VT-VF) as fatal cardiac arrhythmias are the main factors triggering sudden cardiac death. The objective of this study is to find early signs of sustained VT-VF in patients with an implanted cardioverter-defibrillator (ICD). These devices are able to safeguard patients by returning their hearts to a normal rhythm via strong defibrillatory shocks; additionally, they store the 1000 beat-to-beat intervals immediately before the onset of a life-threatening arrhythmia. We study these 1000 beat-to-beat intervals of 17 chronic heart failure ICD patients before the onset of a life-threatening arrhythmia and at a control time, i.e., without a VT-VF event. To characterize these rather short data sets, we calculate heart rate variability parameters from the time and frequency domain, from symbolic dynamics as well as the finite-time growth rates. We find that neither the time nor the frequency domain parameters show significant differences between the VT-VF and the control time series. However, two parameters from symbolic dynamics as well as the finite-time growth rates discriminate significantly both groups. These findings could be of importance in algorithms for next generation ICD's to improve the diagnostics and therapy of VT-VF.

PACS number(s): 87.19.Hh, 05.45.Tp, 02.50.Sk

I. INTRODUCTION

Sudden cardiac death is a major public health problem, accounting for approximately 400 000 deaths in the United States annually [1,2]. Therefore, an accurate and reliable identification of patients who are at high risk of sudden cardiac death is an important and challenging problem. The main factors triggering sudden cardiac death are in most cases either ventricular tachycardia (VT) or ventricular fibrillation (VF), which are connected with transient increases in sympathetic tone [3,4] and based on inter- and intraindividual different risk factors [5,6]. Ventricular tachycardia is defined as three or more consecutive impulses (heartbeats) at a rate exceeding 100/min. The impulses originate in pacemakers located distal to the bifurcation of the bundle of His, in the bundle branches, Prukinje fibers or, rarely, in the working myocardium of the ventricles. During ventricular tachycardia, the heart does not pump blood as efficiently as it does during a normal rhythm. Ventricular fibrillation is a particular type of reentry usually leading to very fast but completely irregular disorganized activation of the entire myocardium of the ventricles. It is more serious than ventricular tachycardia because it causes sudden cardiac death if not treated immediately.

Heart rate variability (HRV) parameters, calculated from the time series of the beat-to-beat-intervals, have been used to predict the mortality risk in patients with structural heart diseases [7,8]. We have recently demonstrated that a multivariate approach with HRV parameters, including nonlinear methods as well as the combination of HRV measures with clinical parameters like the ejection fraction, the complexity of ventricular arrhythmias, or the signal-averaged electrocardiogram, improves the results of risk stratification [9]. Recent studies showed that HRV assesses the autonomic nervous system dysfunction and is able to identify patients at risk of sudden cardiac death [10,11]. However, these methods are not developed to perform short-term predictions of malignant ventricular arrhythmias.

Recently Liebovitch *et al.* [12] discovered that the times between VT-VF events have a power law form, which demonstrates the nonlinear properties of such cardiac arrhythmias. An interesting approach for a short-term prediction of ventricular fibrillation is described in [13], where it is shown that conventional HRV analysis preceding a VT fails to predict imminent VF. Another approach to predict VT-VF is based on critical phases [14], the authors found an increased number of special patterns before VT-VF. Furthermore, Meyerfeldt *et al.* [15] discovered that two basic modes of onset are responsible for monomorphic ventricular tachycardia: one without beat-to-beat-interval variations occurring immediately prior to onset and another characterized by short-long-short sequences and increased QT dispersion. The QT interval is defined as the time between the beginning of ventricular excitation (Q wave) and the end of the heart repolarization (the end of the T wave). The QT dispersion is determined as the difference between the maximum and minimum QT interval in all leads of the surface electrocardiogram.

All these approaches for a short-term prediction of VF/VT are based on linear methods. However, the application of nonlinear methods in addition to the traditional measures of HRV seems to be more promising [9,16–23]. Nevertheless, many nonlinear methods require rather long time series and are not easily applicable to very short data sets as used in this study.

*Electronic address: wessel@fvk-berlin.de

The objective of this contribution is to find early signs of VT-VF in patients with an implanted cardioverter-defibrillator (ICD) to make a short-term prediction possible and consequently to improve antiarrhythmic therapy. The defibrillators are able to safeguard patients by returning their hearts to a normal rhythm via strong defibrillatory shocks. Additionally, they store the 1000 beat-to-beat intervals immediately before the onset of a life-threatening arrhythmia. Therefore, we apply standard HRV parameters from the time and frequency domain [11], parameters from symbolic dynamics [18,19], as well as the finite-time growth rates [24] to the data stored in the ICD.

The paper is organized as follows. In Sec. II we describe the data and standard techniques in the time and frequency domain. In Sec. III we present parameters from nonlinear data analysis based on symbolic dynamics and finite-time growth rates. Section IV contains the results of the data analysis. Finally, in Sec. V we discuss our results.

II. DATA AND STANDARD METHODS

The defibrillators used in this study (PCD 7220/7221, Medtronic) are able to store at least 1000 beat-to-beat intervals prior to onset of VT (10 msec resolution), corresponding to approximately 15 min. We analyze these intervals in 17 chronic heart failure ICD patients (normal sinus rhythm, no class I or III antiarrhythmic drugs) just before the onset of a VT-VF and at a control time, i.e., without a following arrhythmic event. Time series including more than one nonsustained VT, with induced VT's, pacemaker activity, or more than 10% of ventricular premature beats are excluded from this analysis. So that from the 17 patients, 24 tachograms, i.e., the time series of the beat-to-beat intervals, with a subsequent VT-VF and the respective 24 control time series without VT-VF are considered. Note that three patients had already several VT's. To analyze only the dynamics occurring just before a VT, the beat-to-beat intervals of the VT itself at the end of the time series are removed from the tachograms. Figure 1 shows an example of 1000 beat-to-beat intervals just before a sustained VT (with the following VT) as well as a control tachogram of the same patient.

To detect early signs of a life-threatening arrhythmia, we apply a multiparametric analysis. Before starting the analysis ventricular premature beats as well as artifacts should be removed from the time series [25], constructing the so-called normal-to-normal-beat time series (NN). The following standard HRV parameters [11] are calculated from all corrected time series: ''meanNN,'' the mean beat-to-beat interval of the time series; ''sdNN,'' its standard deviation; ''pNN50,'' the percentage of beat-to-beat interval differences greater than 50 msec; and ''rmssd,'' the root mean square of successive beat-to-beat interval differences. Additionally, the standard parameters ''VLF,'' ''LF,'' ''HF,'' and ''P'' from the frequency domain are calculated [11]. ''VLF'' represents the power in the frequency band from 0.0033 to 0.04 Hz; ''LF'' the power from 0.04 to 0.15 Hz; ''HF'' the power from 0.15 to 0.4 Hz; and ''P'' the total power from 0.0033 to 0.4 Hz. The spectra are estimated using the fast Fourier transform. To avoid the ''leakage'' effect, a Blackman-Harris window function is applied. The following ratios are included in our analysis: VLF to P, HF to P, and LF to HF as well as LFn; the normalized low-frequency band. These standard parameters of HRV analysis are based on linear techniques. To classify dynamical changes in the time series, we are using in the following the concepts of symbolic dynamics and the finite-time growth rates.

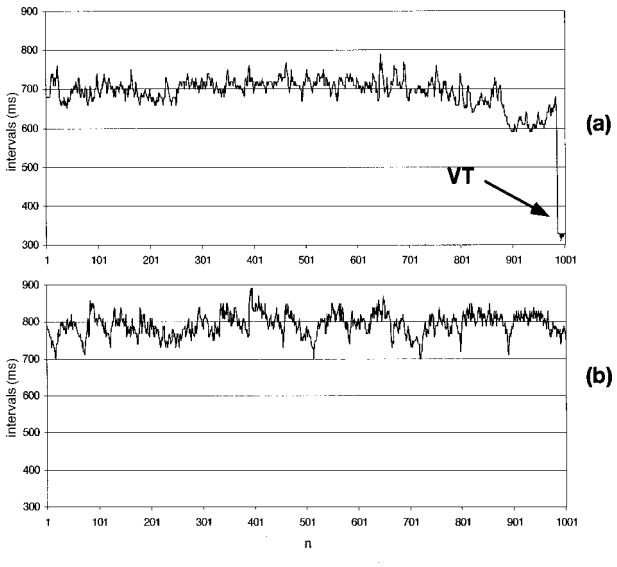

FIG. 1. The last 1000 beat-to-beat intervals before a sustained VT (a) and the respective control time series (b) from the same patient. To analyze the dynamics just before an arrhythmia, all beat-to-beat intervals of the VT itself (starting at the arrow) at the end of time series (a) are removed from the tachograms.

III. NONLINEAR ANALYSIS

A. Symbolic dynamics

We have shown that symbolic dynamics is an efficient approach to analyze dynamic aspects of HRV [18,19]. The first step in this analysis is the transformation of the time series into symbol sequences with symbols from a given alphabet. Some detailed information is lost in this process, but the coarse dynamic behavior can be analyzed. Wackerbauer *et al.* [26] used the methodology of symbolic dynamics for the analysis of the logistic map, where a generic partition is known. However, for physiological time series analysis a more pragmatic approach is necessary. The transformations into symbols have to be chosen context dependent. For this reason, we develop complexity measures on the basis of such context-dependent transformations, which have a close connection to physiological phenomena and are relatively easy to interpret.

Comparing different kinds of symbol transformations, we found that the use of four symbols, as explained in Eq. (1), is appropriate for our purpose. The time series $x_1,x_2,x_3,\ldots,x_N$ is transformed into the symbol sequence $s_1,s_2,s_3,\ldots,s_N$, $s_i \in A$ on the basis of the alphabet $A=\{0,1,2,3\}$. The transformation into symbols refers to three given levels where μ denotes the mean beat-to-beat interval and a is a special parameter that we have chosen 0.05; we tested several values of a from 0.03 to 0.07; however, the resulting symbol sequences differed not significantly,

$$s_i(x_i)=\begin{cases} 0: & \mu & <x_i\leqslant(1+a)\mu \\ 1: & (1+a)\mu & <x_i<\infty \\ 2: & (1-a)\mu & <x_i\leqslant\mu \\ 3: & 0 & <x_i\leqslant(1-a)\mu \end{cases}$$

$$\text{where } i=1,2,3,\ldots . \tag{1}$$

There are several quantities that characterize such symbol strings. In this study we analyze the frequency distribution of length three words, i.e., substrings which consist of three symbols from the alphabet *A*, leading to a maximum of 64 different words (bins). This is a compromise of having, on the one hand, some dynamical information and of having, on the other hand, a sufficient good statistics to estimate the probability distribution. We consider the following measures of complexity.

(i) The Shannon entropy H_k (''fwshannon'' in Table I) calculated from the distribution p of words is the classic measure for the complexity in time series:

$$H_k=-\sum_{\omega\in W^k,p(\omega)>0} p(\omega)\log p(\omega), \tag{2}$$

where W^k is the set of all words of length k. Larger values of Shannon entropy refer to higher complexity in the corresponding tachograms and lower values to lower ones.

(ii) Next, we count the ''forbidden words'' in the distribution of words with length 3—that is the number of words which never occur. A high number of forbidden words stands for a rather regular behavior in the time series. If the time series is highly complex in the Shannonian sense, only a few forbidden words can be found.

(iii) To measure especially low variability, we introduce the parameter ''plvar10.'' In this way successive symbols of another simplified alphabet, consisting only of symbols ''0'' and ''1,'' were analyzed. Here the symbol ''0'' stands for a small difference between two successive beats (the resolution of the defibrillators used in this study), whereas ''1'' represents those cases where the difference between two successive beats exceeds this special limit,

$$s_n=\begin{cases} 1: & |x_n-x_{n-1}|\geqq 10 \text{ msec} \\ 0: & |x_n-x_{n-1}|<10 \text{ msec}. \end{cases} \tag{3}$$

Words consisting only of a unique type of symbol (either all ''0'' or all ''1'') were counted. To get a statistically appropriate estimate of the word distribution, we choose words of length six, where again at maximum 64 different types of words can occur. ''Plvar10'' represents the probability of the word type ''000000'' occurrence and is able to detect even intermittent decreased HRV.

B. Finite-time growth rates

Lyapunov exponents of a dynamical system reflect effective growth rates of infinitesimal uncertainties over an infinite duration. However, time series analysis is restricted to the analysis of finite-time series and thus it is difficult to determine Lyapunov exponents [27–31]. Moreover, the 1000 beat-to-beat intervals form only a very short time series and do not allow estimating global Lyapunov exponents. Therefore, we concentrate on quantifying the state-dependent short-term predictability through finite-time growth rates. Note that these differ from the finite-time Lyapunov exponents defined in [32–36] as well as the finite-time growth rates of [24], both of which require the knowledge of the tangent maps thus giving the equations governing the dynamics. In [36] the significant differences between these quantities are discussed.

Our finite-time growth rates are approximations based on the idea of Wolf *et al.* [28]. Firstly, pseudophase spaces of the system are constructed using delay coordinates [37]. Their dimension is denoted by n and the fixed delay by τ. Next, for each point in this constructed phase space $I_k=[x_k,x_{k+\tau},\ldots,x_{k+(n-1)\tau}]$, $k=1,\ldots,N-(n-1)\tau$ of the measured tachogram $I=[x_1,x_2,\ldots,x_N]$ the nearest neighbor $\overline{I_k}$ is determined. $\overline{I_k}$ is defined as that state which has the minimal Euclidean distance to the I_k. $||I_u-I_v||$ denotes the Euclidean distance of the state I_u to I_v, i.e.,

$$||I_u-I_v||=\sqrt{\sum_{j=0}^{n-1}(x_{u+j\tau}-x_{v+j\tau})^2}. \tag{4}$$

Then the minimal distance d_k to the state I_k is given by

$$d_k=\min_{\substack{i=1,\ldots,N-(n-1)\tau \\ |i-k|>(n-1)\tau}} \|I_k-I_i\|,\quad k=1,\ldots,N-(n-1)\tau \tag{5}$$

and the nearest neighbor by

$$\overline{I_k}=\{I_m|\|I_k-I_m\|=d_k\},k=1,\ldots,N-(n-1)\tau. \tag{6}$$

Note that the time lag of the nearest neighbor has to be at least one window length, i.e., $|i-k|>(n-1)\tau$ and we only consider points as neighbors if their distance to the base point is less than 10% of the maximum distance between any two points. Next, we analyze the evolution of the states I_k and $\overline{I_k}$ during the time T. After these T steps we get the states $I_k^T=[x_{k+T},x_{k+T+\tau},\ldots,x_{k+T+(n-1)\tau}]$ and $\overline{I_k^T}$, respectively. The distance between both states $\|I_k^T-\overline{I_k^T}\|$ represents the divergence after T evolution steps. From the original distance of both states and the distance after T steps we calculate the finite-time growth rate $\lambda_k^{(n,\tau,T)}$:

$$\lambda_k^{(n,\tau,T)}=\frac{1}{T}\ln\frac{\|I_k^T-\overline{I_k^T}\|}{\|I_k-I_k'\|},k=1,\ldots,N-(n-1)\tau. \tag{7}$$

$\lambda_k^{(n,\tau,T)}$ quantifies the local short-term predictability at the point I_k. If these $\lambda_k^{(n,\tau,T)}$ are greater than zero, the distance after the evolution time increases; otherwise, it decreases.

We calculate the finite-time growth rates for each point of the delay phase space, which leads to a growth rate time series $\lambda_k^{(n,\tau,T)}$. Its average, the average growth rate $\lambda^{(n,\tau,T)}$,

$$\lambda^{(n,\tau,T)}=\frac{1}{N-(n-1)\tau+1}\sum_{k=1}^{N-(n-1)\tau}\lambda_k^{(n,\tau,T)} \tag{8}$$

quantifies a global short-term predictability. The dimension n, i.e., the length of the selected tachogram part varied from 3 to 9. We choose this range to cover an interval up to 9, which is a typical order of an autoregressive model for short-term HRV tachograms [25]. The evolution time and the delay are defined as $T=1,2,3$ and $\tau=1,2,3$, respectively.

Additionally, to reduce random influences, we consider a three- and a five-nearest-neighbors approach. According to Eq. (6) we determine the five nearest neighbors $\overline{I_k^1}, \ldots, \overline{I_k^5}$ of the point I_k and evolve all neighbors over the evolution time T. The finite-time growth rates for the three- and the five-nearest-neighbors approaches are derived from the average distances before and after the evolution time.

IV. RESULTS

We calculate the parameters described in the preceding sections for both the VT-VF and the control time series and test then for equality of the averaged values obtained from both groups. The statistical analysis is based on the two-tailed t test and the nonparametric Kolmogorov-Smirnov Z test.

Firstly, the standard parameters in the time and frequency domain are determined. We find that none of them leads to a significant separation of both groups (Table I). As already visible in Fig. 1, the mean beat-to-beat interval meanNN showed a remarkable but nonsignificant difference between the groups.

On the contrary, two parameters of symbolic dynamics (''fwshannon'' and ''plvar10'', see Table II) as well as the finite-time growth rates indicate significant differences between both groups. The Shannon entropy of the word distribution ''fwshannon'' is significantly higher in the control group, whereas the short-variability measure ''plvar10'' is higher in the VT-VF group. Both parameters indicate a partly decreased heart rate variability in the VT-VF group which cannot be shown with the standard deviation ''sdNN'' or other variability measures from time domain. It is interesting to note that the forbidden word statistics fail to distinguish both groups.

TABLE I. Time and frequency domain parameters before VT-VF and at control time (p significance; n.s., not significant, $p \geqslant 0.05$). The statistical analysis is based on the two-tailed t test and on the nonparametric Kolmogorov-Smirnov Z test; the parameter values are expressed as mean ± standard deviation.

	VT-VF	Control	p
	Time domain		
meanNN	697.1±155.6	756.3±149.9	n.s.
sdNN	54.07±40.62	55.10±33.47	n.s.
pNN50	0.02±0.04	0.04±0.11	n.s.
rmssd	14.85±10.30	20.52±20.36	n.s.
	Frequency domain		
VLF to *P*	0.54±0.16	0.52±0.17	n.s.
LF to *HF*	4.18±4.07	3.36±1.42	n.s.
HF to *P*	0.04±0.04	0.05±0.04	n.s.
LFn	0.74±0.13	0.75±0.09	n.s.

TABLE II. Parameters from symbolic dynamics and finite time growth rates calculated for dimensions three, six, and nine with delay $\tau=1$ and evolution time $T=1$ before VT-VF and at control time (five-nearest-neighbor approach; p, significance; n.s., not significant; $p \geqslant 0.05$)

	VT-VF	Control	p
	Symbolic dynamics		
forbword	32.2±10.5	32.1±9.3	n.s.
fwshannon	2.13±0.59	2.43±0.43	0.036
plvar10	0.12±0.18	0.04±0.05	0.032
	Finite-time growth rates		
$\lambda^{(3,1,1)}$	0.37±0.31	0.51±0.36	n.s.
$\lambda^{(6,1,1)}$	0.22±0.08	0.26±0.05	0.044
$\lambda^{(9,1,1)}$	0.11±0.03	0.13±0.02	0.030

The finite-time growth rates were calculated for the single, the three-, and the five-nearest-neighbors approaches. Table II represents the mean values and standard deviations of $\lambda^{(n,\tau,T)}$ for the VT-VF group as well as for the control group in the five-nearest-neighbors approach ($n=3,6,9$, $\tau=1$, $T=1$). The parameter $\lambda^{(3,1,1)}$ denotes the average growth rate with a dimension of 3, lag 1, and evolution time 1, $\lambda^{(6,1,1)}$, $\lambda^{(9,1,1)}$, respectively. For dimension three there are no significant differences, whereas the average growth rates for dimensions six and nine differed significantly in both groups. For evolution times $T=2,3$ significant differences disappeared for a dimension of 6. Interestingly, for all dimensions the growth rates were larger in the group of the control tachograms than in the VT-VF group.

Additionally, we calculated the average growth rates for different delay times $\tau=2,3$, evolution time $T=1$, and dimensions three to nine. For delay 2 we found a significant difference for a dimension of 6 ($\lambda^{(6,2,1)}$, $p=0.016$). For delay 3 we only recognized a considerable but nonsignificant difference for $\lambda^{(6,2,1)}$ ($p=0.052$), no further growth rates showed significant differences between both investigated groups.

To estimate the dependence of the results on the time series length, we calculate all parameters ($\tau=1$, $T=1$) for the shortened time series; the first 2, 4, and 6 min (this corresponds to approximately 150, 300, and 450 beats) of the time series were disregarded. As a result all significant differences obtained from the complete time series remain valid. This is a strong indication that heart rate variability changes occur a few minutes before a malignant arrhythmia.

To get an overview of the nearest neighbors distance, we calculated the maximum distance between any two points (md) and for each point the distance to its nearest neighbor (dnn). This also was done for the five-nearest-neighbors approach, for dimensions $n=3,\ldots,9$ and with delay $\tau=1$. Table III represents the mean values as well as the 95%-confidence intervals of these distances. A ratio of 8% of both distances dnn/md may be considered as rather large; however, such values appear to be typical for noisy short time series.

The results of the three-nearest-neighbors approach are similar to the five-nearest-neighbors approach. For all selected delays $\tau=1,2,3$ we got significant differences for the

TABLE III. Nearest-neighbor statistics calculated for dimensions $n=3,6,9$ and with delay $\tau=1$ (five-nearest-neighbors approach). The parameter values md, the maximum distance between any two points, and dnn, the distance to the nearest neighbor, are given as mean value and 95%-confidence interval (CI), respectively.

n	md	dnn	dnn/md
3	278.81 (95% CI 235.00-322.63)	6.15 (95% CI 4.36-7.94)	0.022
6	373.17 (95% CI 312.92-433.41)	20.11 (95% CI 15.22-24.99)	0.054
9	436.18 (95% CI 364.14-508.21)	32.86 (95% CI 25.04-40.68)	0.075

average finite-time growth rates (dimension nine). In the single-nearest-neighbor approach no significant differences between the investigated groups were found.

To detect early signs of a life-threatening arrhythmia, we have applied a multiparametric analysis, calculating (i) standard time and frequency parameters, (ii) parameters from symbolic dynamics, as well as (iii) the finite-time growth rates with different dimensions and delays. Analyzing the significance such a large number of parameters leads to a multiple-testing problem: If the tests are treated as independent then the probability of rejecting a valid null hypothesis increases with the number of tests performed. If the number of significant differences between control and VT-VF is an artifact due to multiple testing, we would expect to find approximately the same number of significant differences in surrogate data [38], in which the nonlinearities are destroyed. Therefore, for each time series in our study an amplitude-adjusted surrogate [39] series was created, where the histogram of the surrogate time series is the same as that of the original data. Moreover, the surrogate data is simply a sorted version of the original data, but the sorting procedure is performed in a very careful way that attempts to match the autocorrelation function of the original data. Figure 2 gives two examples of surrogate data calculated from the time series demonstrated in Fig. 1. All parameters introduced above were tested for different mean values between the surrogate

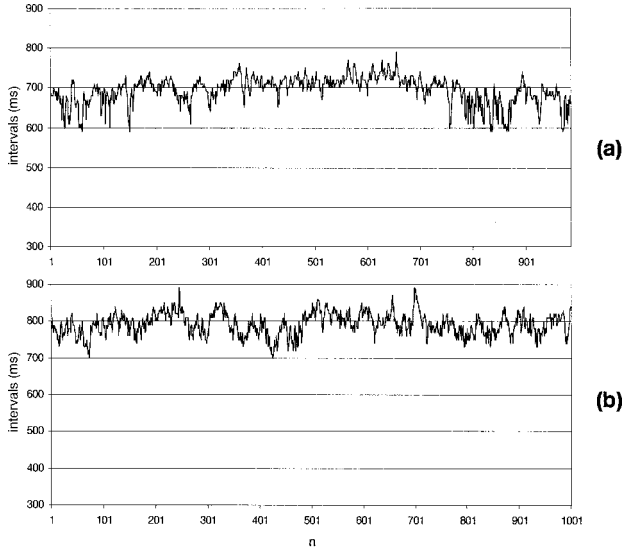

FIG. 2. Amplitude adjusted surrogates of the 1000 beat-to-beat intervals before a sustained VT of Fig. 1(a) (without the VT beats) (a) and of the respective control time series from Fig. 1(b) of the same patient (b).

VT and the surrogate control time series. However, no parameter showed significant differences between both groups (see Table IV). This result is an indication that the differences achieved above are not artifacts due to multiple tests.

To investigate the strength of the relationship between the finite-time growth rates and parameters from symbolic dynamics the correlation coefficients were calculated. The absolute value of the correlation coefficient between $\lambda^{(n,1,1)}$, $n=3,6,9$ and ''fwshannon'' was on average 0.3, between $\lambda^{(n,1,1)}$, $n=3,6,9$ and ''plvar10'' on average 0.35. Therefore, the combined use of symbolic dynamics parameters and finite-time growth rates may improve the identification of potentially following imminent arrhythmias. In this study there was only a slow increase in discriminating both groups of time series; it has to be validated on a larger data base.

V. DISCUSSION

The aim of this study is to find heart rate variability changes just before the onset of ventricular tachycardia or ventricular fibrillation, i.e., to look for some precursorlike activities before this qualitative change. Two approaches from nonlinear dynamics indeed exhibit significant changes of heart rate variability: methods of symbolic dynamics and finite-time growth rates. It is important to note that standard linear techniques are not able to discriminate between these both groups.

From finite-time growth rates we get significant differences between the VT-VF and the control time series only for relative high dimension ($n>5$). This indicates that the

TABLE IV. Results of the surrogate analysis parameters from symbolic dynamics and finite time growth rates calculated for dimensions three, six, and nine with delay $\tau=1$ and evolution time $T=1$ before VT-VF and at control time (five-nearest-neighbors approach; p, significance; n.s., not significant; $p\geqslant 0.05$)

	VT-VF	Control	p
	Symbolic dynamics		
forbword	34.1 ± 10.1	39.9 ± 11.0	n.s.
fwshannon	2.44 ± 0.41	2.63 ± 0.41	n.s.
plvar10	0.03 ± 0.04	0.01 ± 0.01	n.s.
	Finite-time growth rates		
$\lambda^{(3,1,1)}$	0.63 ± 0.29	0.74 ± 0.28	n.s.
$\lambda^{(6,1,1)}$	0.30 ± 0.04	0.31 ± 0.04	n.s.
$\lambda^{(9,1,1)}$	0.14 ± 0.02	0.14 ± 0.01	n.s.

changes are mainly caused by sympathetic activities of the autonomous nervous system. Vagal activities would cause smaller dimensions. These results are in good agreement with the physiological fact that the sympathetic activity increases before the onset of VT [3,4].

The significant lower values of $\lambda^{(n,1,T)}$, $n=6,9$, $T=1,2,3$ in the VT-VF group provide a possibility to predict a VT-VF. The calculation of $\lambda^{(n,\tau,T)}$ with different delays τ has shown the importance of analyzing beat-to-beat variability, no successive heart beats should be removed. For delays greater than one, significant differences in the average growth rates decreased, which shows that the differences between the VT-VF time series and the controls are caused by beat-to-beat regulation.

The nearest-neighbor statistics was useful for assessing the results. Dimensions higher than nine should not be used; the nearest neighbors could be only distantly related. A quotient less than 0.1 of the nearest neighbor distance to the maximum distance between any two points (dnn/md) seems to be normal for these short physiologic time series with stochastic influences.

The methods of symbolic dynamics are useful approaches for classifying the dynamics of heart rate variability. By means of these methods, the underlying dynamics of the time series can be investigated. Parameters of the time and frequency domain often leave these dynamics out of consideration. The optimized symbol definition has to be validated on a more representative number of patients. It is necessary to check which symbol definition best describes the dynamical changes inherent in the time series just before the onset of a malignant arrhythmia. However, symbolic dynamics is a method with a very close connection to physiological phenomena and is relatively easy to interpret.

The results of the correlation analysis showed that the parameters from symbolic dynamics and the new derived methods are only weakly correlated; the combination of all methods may improve the discrimination of VT-VF and control time series. However, the relative small data base we used in this study does not allow multivariate analyses.

Moreover, this study demonstrated the advantage of using methods from nonlinear dynamics. The evolution of points in phase space provides a deeper insight into dynamical aspects of the cardiac system. The importance of beat-to-beat analysis under consideration of the time series order was shown.

Limitations of this study are the relatively small number of time series and the reduced statistical analysis (no subdivisions concerning age, sex, and heart disease). For this reason, these results have to be validated on a larger data base. Furthermore, this investigation could be enhanced for tachograms including more than 10% ventricular premature beats.

In conclusion, this study demonstrated that parameters from nonlinear dynamics could be meaningful for the prediction of VT-VF events even in short term HRV time series. This finding seems to be of importance in algorithms for risk stratification and to improve the therapeutic and preventive tools of next generation ICD's.

ACKNOWLEDGMENTS

This work was supported by grants from the Federal Ministry of Education, Science, Research and Technology BMBF (13N7113/5) and the Deutsche Forschungsgemeinschaft DFG (vo505-2/1).

[1] R. J. Damiano, Jr., J. Cardiovasc. Surg. **7**, 36 (1992).
[2] H. V. Barron and M. D. Lesh, J. Am. Coll. Cardiol. **27**, 1053 (1996).
[3] B. B. Lerman, K. Stein, E. D. Engelstein, D. S. Battleman, N. Lippman, D. Bei, and D. Catanzaro, Circulation **92**, 421 (1995).
[4] K. M. Stein, L. A. Karagounis, J. L. Anderson, P. Kligfield, and B. B. Lerman, Circulation **91**, 722 (1995).
[5] S. H. Hohnloser, T. Klingenheben, A. van de Loo, E. Hablawetz, H. Just, and P. J. Schwartz, Circulation **89**, 1068 (1994).
[6] J. E. Hartikainen, M. Malik, A. Staunton, J. Poloniecki, and A. J. Camm, J. Am. Coll. Cardiol. **28**, 296 (1996).
[7] R. E. Kleiger, J. P. Miller, J. T. Bigger, Jr., and A. J. Moss, Am. J. Cardiol. **59**, 256 (1987).
[8] H. Tsuji, M. G. Larson, F. J. Venditti, Jr., E. S. Manders, J. C. Evans, C. L. Feldman, and D. Levy, Circulation **94**, 2850 (1996).
[9] A. Voss, K. Hnatkova, N. Wessel, J. Kurths, A. Sander, A. Schirdewan, A. J. Camm, and M. Malik, Pac. Clin. Electrophysiol. **21**, 186 (1998).
[10] L. Fei, M. H. Anderson, D. J. Statters, M. Malik, and A. J. Camm, Am. Heart J. **129**, 285 (1995).
[11] Task Force of the European Society of Cardiology and the North American Society of Pacing and Electrophysiology, Circulation **93**, 1043 (1996).
[12] L. S. Liebovitch, A. T. Todorov, M. Zochowski, D. Scheurle, L. Colgin, M. A. Wood, K. A. Ellenbogen, J. M. Herre, and R. C. Bernstein, Phys. Rev. E **59**, 3312 (1999).
[13] T. Vybiral, D. H. Glaeser, A. L. Goldberger, D. R. Rigney, K. R. Hess, J. Mietus, J. E. Skinner, M. Francis, and C. M. Pratt, J. Am. Coll. Cardiol. **22**, 557 (1993).
[14] L. Karolyi, T. Hilbel, T. Beyer, W. Schöls, and J. Brachmann, Z. Kardiol. **86**, 33 (1997).
[15] U. Meyerfeldt, A. Schirdewan, M. Wiedemann, H. Schutt, F. Zimmerman, F. C. Luft, and R. Dietz, Eur. Heart J. **18**, 1956 (1997).
[16] A. L. Goldberger, D. R. Rigney, J. Mietus, E. M. Antman, and S. Greenwald, Experientia **44**, 983 (1988).
[17] L. Glass and D. Kaplan, Med. Prog. Technol. **19**, 115 (1993).
[18] J. Kurths, A. Voss, A. Witt, P. Saparin, H. J. Kleiner, and N. Wessel, Chaos **5**, 88 (1995).
[19] A. Voss, J. Kurths, H. J. Kleiner, A. Witt, N. Wessel, P. Saparin, K. J. Osterziel, R. Schurath, and R. Dietz, Cardiovasc. Res. **31**, 419 (1996).
[20] Th. Schreiber, Phys. Rev. Lett. **78**, 843 (1997).
[21] T. H. Makikallio, T. Seppanen, K. E. Airaksinen, J. Koistinen, M. P. Tulppo, C. K. Peng, A. L. Goldberger, and H. V. Huikuri, Am. J. Cardiol. **80**, 779 (1997).
[22] C. Schäfer, M. G. Rosenblum, J. Kurths, and H. H. Abel, Nature (London) **392**, 239 (1998).
[23] P. I. Saparin, M. Zaks, J. Kurths, A. Voss, and V. Anishchenko, Phys. Rev. E **54**, 737 (1996).
[24] J. M. Nese, Physica D **35**, 237 (1989).
[25] N. Wessel, A. Voss, J. Kurths, P. Saparin, A. Witt, H. J. Kleiner, and R. Dietz, in *Computers in Cardiology 1994* (IEEE

Computer Society Press, Los Alamitos, 1996), p. 137.
[26] R. Wackerbauer, A. Witt, H. Atmanspacher, J. Kurths, and H. Scheingraber, Chaos Solitons Fractals **4**, 133 (1994).
[27] V. I. Oseledec, Trans. Moscow Math. Soc. **19**, 197 (1968).
[28] A. Wolf, J. B. Swift, H. L. Swinney, and J. A. Vastano, Physica D **16**, 285 (1985).
[29] J. P. Eckmann, S. Oliffson Kamphorst, D. Ruelle, and S. Ciliberto, Phys. Rev. A **34**, 4971 (1986).
[30] J. Kurths and H. Herzel, Physica D **25**, 165 (1987).
[31] L. A. Smith, Philos. Trans. R. Soc. London, Ser. A **348**, 371 (1994).
[32] E. N. Lorenz, Tellus **17**, 321 (1965).
[33] H. D. I. Abarbanel, R. Brown, and M. B. Kennel, Int. J. Mod. Phys. B **5**, 1347 (1991).
[34] R. Brown, P. Bryant, and H. D. I. Abarbanel, Phys. Rev. A **43**, 2787 (1991).
[35] S. Yoden and M. Nomura, J. Atmos. Sci. **50**, 1531 (1993).
[36] C. Ziehmann, L. A. Smith, and J. Kurths, Physica D **126**, 49 (1999).
[37] F. Takens, in *Dynamical Systems and Turbulence*, edited by D. Rand and L. S. Young (Springer-Verlag, Berlin, 1981), p. 366.
[38] M. R. Allen and L. A. Smith, J. Clim. **9**, 3373 (1996).
[39] J. Theiler, S. Eubank, A. Longtin, B. Galdrikian, and J. D. Farmer, Physica D **58**, 77 (1992).